2001

Mon. Not. R. Astron. Soc. **000**, 2–14 (2001)

General Relativistic Electromagnetic Fields of a Slowly Rotating Magnetized Neutron Star. II. Solution of the Induction Equations

Olindo Zanotti[(1)] and Luciano Rezzolla[(1),(2)]

[(1)] *SISSA, International School for Advanced Studies, Via Beirut, 2-4 34014 Trieste, Italy*
[(2)] *INFN, Department of Physics, University of Trieste, Via A. Valerio, 2 34127 Trieste, Italy*

4 December 2001

ABSTRACT

We have solved numerically the general relativistic induction equations in the interior background spacetime of a slowly rotating magnetized neutron star. The analytic form of these equations was discussed in a recent paper (Rezzolla *et al* 2001a), where corrections due both to the spacetime curvature and to the dragging of reference frames were shown to be present. Through a number of calculations we have investigated the evolution of the magnetic field with different rates of stellar rotation, different inclination angles between the magnetic moment and the rotation axis, as well as different values of the electrical conductivity. All of these calculations have been performed for a constant temperature relativistic polytropic star and make use of a consistent solution of the initial value problem which avoids the use of artificial analytic functions. Our results show that there exist general relativistic effects introduced by the rotation of the spacetime which tend to *decrease* the decay rate of the magnetic field. The rotation-induced corrections are however generally hidden by the high electrical conductivity of the neutron star matter and when realistic values for the electrical conductivity are considered, these corrections become negligible even for the fastest known pulsar.

Key words: relativity – stars: neutron – rotation – magnetic fields

1 INTRODUCTION

Irrespective of the origin of magnetic fields in neutron stars, whether produced by thermoelectric effects active in a thin layer below the star surface when the temperature is much above 10^6K (see, for instance, Wiebicke & Geppert, 1996), or by a dynamo action during the earliest stages of the convective motions (see Thompson & Duncan, 1993), or by post core-collapse accretion of fall-back material after a supernova explosion giving rise to a neutron star, a secular decay of the magnetic field is expected as a result of the finite electrical conductivity of the stellar matter. The theoretical research in this area is intense, pushed on by the observational evidence that magnetic fields in neutron stars are decreasing with increasing spin-down age. There is now a general consensus about the possibility of improving the present knowledge of the internal structure of neutron stars by using the constraints from observations of the magnetic field decay. This justifies the effort of taking into account all of the possible factors which are supposed to play a role during the decay of the magnetic field.

Particularly interesting within this context are the general relativistic corrections induced by the presence of a strongly curved background spacetime. These corrections have been investigated by a number of authors (Ginzburg & Ozernoy 1964, Anderson & Cohen 1970, Petterson 1974, Gupta *et al* 1998, Konno & Kojima 2000) and with a number of different approaches some of which are more rigorous (Geppert *et al*, 2000) than others (Sengupta 1995, 1997). In recent related works, Rezzolla *et al* (2001a, 2001b) have performed a detailed analysis of Maxwell's equations in the external and internal background spacetime of a rotating magnetized conductor. As a result of this analysis, it was possible to show that in the case of finite electrical conductivity, general relativistic corrections due both to the spacetime curvature and to the dragging of reference frames are present in the induction equations. Moreover, when the stellar rotation is taken into account, each component of the magnetic field is governed by its own evolutionary law, thus removing the degeneracy encountered in the case of nonrotating spacetimes. The purpose of this paper, which is the natural extension of the work in Rezzolla *et al* (2001a, hereafter paper I), is to quantify the general relativistic effects related to rotation on the evolution of the magnetic field. We have therefore solved numerically the general relativistic induction equations derived in Paper I for a relativistic polytropic star with different values of the rotation period and of the electrical conductivity. Each of the several calculations performed here benefits from the consistent solution of the initial value problem

for a magnetic field which is initially permeating a perfectly conducting relativistic star. This approach avoids the use of artificial initial data and provides a more accurate solution of the induction equations.

Overall, our results show that the rotation of the star and of the background spacetime introduce a *decrease* in the decay rate of the magnetic field. In general, however, the rotation-induced corrections are hidden by the high electrical conductivity of the neutron star matter and are effectively negligible even for the fastest known pulsar. Also in the absence of rotation, the spacetime curvature introduces modifications to the evolution of the magnetic field when compared with the corresponding evolution in a flat spacetime. These modifications depend sensitively on both the metric functions of the interior spacetime and on the radial profile of the electrical conductivity. In the case the star is modeled as a polytrope and the electrical conductivity is assumed to be uniform in space and time, the spacetime curvature generally increases the decay rate of the magnetic field as compared to the flat spacetime case, with this increase being dependent on the compactness of the star.

The paper is organized as follows: in Section 2 we discuss our treatment of the internal structure of the star in the limit of slow rotation. Section 3 is devoted to the solution of the induction equations derived in paper I, with some emphasis on the numerical aspects and in particular on the initial value problem. We show our results in Section 4, whereas Section 5 contains the conclusions. Throughout, we use a space-like signature $(-,+,+,+)$ and a system of units in which $G = c = M_\odot = 1$ (However, for those expressions of astrophysical interest, we have written the speed of light explicitly.). Partial spatial derivatives are denoted with a comma.

2 STELLAR STRUCTURE

The background metric of a stationary, slowly-rotating star at first order in the angular velocity Ω, is given by

$$ds^2 = -e^{2\Phi(r)}dt^2 + e^{2\Lambda(r)}dr^2 - 2\omega(r)r^2\sin^2\theta dt d\phi + r^2\sin^2\theta d\phi^2, \tag{1}$$

where $\omega(r)$ is the angular velocity of a free-falling inertial frame. For realistic values of the stellar magnetic field (i.e. $B = 10^{11} - 10^{13}$ G) we can neglect the contribution of the electromagnetic fields to the background spacetime geometry and determine the internal structure of the star and its interior spacetime after solving the following system of ordinary differential equations (henceforth TOV system, from Tolmann, 1939; Oppenheimer & Volkoff, 1939)

$$\begin{aligned} \frac{dp}{dr} &= -\frac{(p+e)(m+4\pi r^3 p)}{r^2(1-2m/r)}\,, \\ \frac{dm}{dr} &= 4\pi r^2 e\,, \\ \frac{d\Phi}{dr} &= \frac{m+4\pi r^3 p}{r^2(1-2m/r)} = -\frac{1}{e}\frac{dp}{dr}\left(1+\frac{p}{e}\right)^{-1}\,, \end{aligned} \tag{2}$$

where $p(r)$ is the pressure, $e(r)$ is the energy density and $m(r)$ is the mass enclosed within r. Once an equation of state has been chosen, the TOV system can be solved numerically together with the differential equation for the Lense-Thirring angular velocity $\omega(r)$ in the internal region of the star

$$\frac{1}{r^3}\frac{d}{dr}\left[r^4 e^{-(\Phi+\Lambda)}\frac{d\bar{\omega}}{dr}\right] + 4\frac{d(e^{-(\Phi+\Lambda)})}{dr}\bar{\omega} = 0\,, \tag{3}$$

where $\bar{\omega} \equiv \Omega - \omega$. After selecting a value for the central rest-mass density, the set of differential equations (2)–(3) is solved from the centre of the star until the pressure vanishes, thus determining the radius R. For the integration of eq. (3), the solution near the centre of the star is simplified if we use the analytic power series expansion $\bar{\omega}/\bar{\omega}_c \simeq 1 + 8\pi(e_c + p_c)r^2/5$, valid for $r \to 0$ and where the label "c" refers to a quantity at the centre of the star (Miller, 1977). Since in the vacuum region of spacetime external to the star $\omega(r) = 2J/r^3$, with J being the total angular momentum, we can determine the two unknown quantities J and ω_c by imposing continuity of the angular velocity and of its first derivative at the surface.

The interior of the star influences the magnetic evolution either macroscopically, by affecting the metric quantities which enter the induction equations, or microscopically, through the electrical conductivity σ which, in turn, depends on the star's temperature and chemical composition (see Urpin & Konenkov, 1997; Page *et al* 2000). Our attention is here mainly focussed on assessing the contribution coming from rotational effects in general relativity on the decay of the magnetic field *. As a consequence, we will neglect the thermal and rotational evolution of the neutron star and simply consider a constant in time and uniform in space electrical conductivity. This is an approximation, but a necessary one to disentangle the many different effects that intervene in the general relativistic evolution of the magnetic field. Furthermore, as will be discussed in Section 4, the assumption of a uniform electrical conductivity does not affect the role of a rotating background spacetime in the evolution of the magnetic field.

We model our relativistic stars as polytropes with equation of state

$$p = K\rho^{1+1/N}\,, \tag{4}$$

* It should be mentioned that general relativistic corrections can appear also in the constitutive relations of the Maxwell equations, such as in the general relativistic form of Ohm's law (Ahmedov 1999). These corrections are usually negligible in the electrodynamics of relativistic stars and will be neglected here.

where ρ, K, N are the rest-mass density, the polytropic constant and the polytropic index, respectively. As "fiducial" model of neutron star we consider a polytrope with index $N = 1$, polytropic constant $K = 100$, and central rest-mass density $\rho_c = 1.28 \times 10^{-3}$. In this case, the radius R and the total mass M obtained through the solution of the TOV system are respectively $R = 14.15$ Km and $M = 1.40\ M_\odot$, yielding a compactness ratio $\eta = 0.29$. The rotation period usually chosen for this model is $P = 10^{-3}$ s.

3 EVOLUTION OF THE INTERNAL MAGNETIC FIELD

As mentioned in the Introduction, the presence of the stellar rotation lifts the degeneracy found in the case of a nonrotating star (Geppert *et al* 2000) and three distinct induction equations regulate the general relativistic evolution of the magnetic field. In this Section we discuss the solution of the induction equations for each of the magnetic field components. The main difficulties encountered in the numerical solution are related to the definition of a consistent initial value problem and to the complex nature of the partial differential equations when a misalignment between the rotation axis and the magnetic dipole moment is present. In the following we discuss the strategies adopted to handle these difficulties.

3.1 The Relativistic Induction Equations

The induction equations for the magnetic field of a slowly rotating relativistic star with finite electrical conductivity have been derived in paper I and we briefly recall them here for completeness. All the measurements are performed in the orthonormal tetrad frame of a "zero angular momentum observer" (ZAMO) and we assume that the spatial components of the magnetic field four-vector in this frame are solutions of the Maxwell equations in the separable form

$$B^{\hat{r}}(r,\theta,\phi,\chi,t) = F(r,t)\Psi_1(\theta,\phi,\chi,t)\,, \tag{5}$$

$$B^{\hat{\theta}}(r,\theta,\phi,\chi,t) = G(r,t)\Psi_2(\theta,\phi,\chi,t)\,, \tag{6}$$

$$B^{\hat{\phi}}(r,\theta,\phi,\chi,t) = H(r,t)\Psi_3(\phi,\chi,t)\,, \tag{7}$$

where F, G, H and Ψ_1, Ψ_2, Ψ_3 account for the radial and angular dependences, respectively. Here, χ is the inclination angle of the stellar magnetic dipole moment relative to the rotation axis and the time dependence in F, G, H is here due to the fact that we are not considering an infinite electrical conductivity but are allowing the magnetic dipole moment to vary in time.

At first order in Ω, the angular eigenfunctions Ψ_i are not affected by general relativistic corrections and assume the flat spacetime expressions

$$\Psi_1 = \cos\chi\cos\theta + \sin\chi\sin\theta\cos\lambda(t)\,, \tag{8}$$

$$\Psi_2 = \cos\chi\sin\theta - \sin\chi\cos\theta\cos\lambda(t)\,, \tag{9}$$

$$\Psi_3 = \sin\chi\sin\lambda(t)\,, \tag{10}$$

where $\lambda(t) \equiv \phi - \Omega t$ is the instantaneous azimuthal position (see Fig. 1 of paper I). Assuming that the contribution of electric currents are negligible[†] the general relativistic evolution equations for the radial eigenfunctions $F(r,t)$, $G(r,t)$, $H(r,t)$ are

$$\begin{aligned}\frac{\partial F}{\partial t}\Psi_1\sin\theta \;=\; & \frac{c^2 e^{-\Lambda}}{4\pi\sigma r^2}\Bigg\{\left[e^{\Phi} r\,(G-H)\right]_{,r}\sin\chi\cos\lambda - 2\left[\left(e^{\Phi} rG\right)_{,r} + e^{\Phi+\Lambda}F\right]\Psi_1\sin\theta \\ & -\frac{1}{4\pi\sigma}\sin\chi\sin\lambda\Bigg\{\left[\omega r(H-G)\right]_{,r}\left(1-2\sin^2\theta\right) + 2\omega e^{-\Phi}\left[\left(e^{\Phi} rH\right)_{,r} + e^{\Phi+\Lambda}F\right]\sin^2\theta \\ & -\Omega r\,(G-H)\,\Phi_{,r}\left(1-2\sin^2\theta\right)\Bigg\}\Bigg\}\,,\end{aligned} \tag{11}$$

[†] Because the magnetic field decay is studied on timescales that are much longer than the electromagnetic wave crossing time, this is a very good approximation.

$$\frac{\partial G}{\partial t}\Psi_2 = \frac{c^2}{4\pi\sigma r}\left\{\frac{e^{\Phi}(G-H)}{r\sin^2\theta}\cos\theta\sin\chi\left[\cos\lambda+\frac{\omega e^{-\Phi}}{4\pi\sigma}\sin\lambda\right]+e^{-\Lambda}\left[e^{-\Lambda}\left(e^{\Phi}rG\right)_{,r}+e^{\Phi}F\right]_{,r}\Psi_2\right.$$
$$\left.-\frac{e^{-\Lambda}}{4\pi\sigma}\cos\theta\sin\chi\sin\lambda\left\{e^{-\Lambda}\left[\omega r(G-H)\right]_{,r}+\omega\left[F+e^{-(\Lambda+\Phi)}\left(re^{\Phi}H\right)_{,r}\right]+\Omega\left[\Phi_{,r}e^{-\Lambda}r(G-H)\right]\right\}_{,r}\right\}, \tag{12}$$

$$\frac{\partial H}{\partial t}\sin\lambda = \frac{c^2e^{-\Lambda}}{4\pi\sigma r}\left\{\left[e^{-\Lambda}\left(e^{\Phi}rH\right)_{,r}+e^{\Phi}F\right]\left[\sin\lambda-\frac{\omega e^{-\Phi}}{4\pi\sigma}\cos\lambda\right]\right\}_{,r}+\frac{c^2e^{\Phi}(G-H)}{4\pi\sigma r^2\sin^2\theta}\left[\sin\lambda-\frac{\omega e^{-\Phi}}{4\pi\sigma}\cos\lambda\right]. \tag{13}$$

Together with the evolution equations (11)–(13), the scalar functions F, G, and H also satisfy the constraint condition of zero-divergence for the magnetic field

$$\left[\left(r^2F\right)_{,r}+2e^{\Lambda}rG\right]\sin\theta\left(\cos\chi\cos\theta+\sin\chi\sin\theta\cos\lambda\right)+e^{\Lambda}r(H-G)\sin\chi\cos\lambda=0\,. \tag{14}$$

A rapid look at equations (11)–(13) shows that in a rotating spacetime the evolution of the poloidal and toroidal components are correlated and that an initially purely poloidal magnetic filed can gain a toroidal component during its evolution and vice-versa. In the case of a nonrotating star, on the other hand, the three induction equations (11)–(13) are not independent and the magnetic field evolution is described by a single scalar function: F (see Geppert et al. 2000).

3.2 Strategy of the Numerical Solution

The numerical solution of equations (11)–(13) is simplified if done in terms of the new quantities

$$\widetilde{F}\equiv r^2F\,, \tag{15}$$

$$\widetilde{G}\equiv e^{\Phi}rG\,, \tag{16}$$

$$\widetilde{H}\equiv e^{\Phi}rH\,, \tag{17}$$

which, when the inclination angle χ is nonzero and the electrical conductivity is uniform, allow us to rewrite eqs. (11)–(13) schematically as

$$\frac{\partial\widetilde{F}}{\partial t}=f_1\widetilde{F}_{,rr}+f_2\widetilde{F}_{,r}+f_3\widetilde{F}+f_4\widetilde{H}_{,r}+f_5\widetilde{G}+f_6\widetilde{G}_{,r}\,, \tag{18}$$

$$\frac{\partial\widetilde{G}}{\partial t}=g_1\widetilde{G}_{,rr}+g_2\widetilde{G}_{,r}+g_3\widetilde{G}+g_4\widetilde{F}_{,r}+g_5\widetilde{F}+g_6\widetilde{H}_{,r}+g_7\widetilde{H}\,, \tag{19}$$

$$\frac{\partial\widetilde{H}}{\partial t}=h_1\widetilde{H}_{,rr}+h_2\widetilde{H}_{,r}+h_3\widetilde{H}+h_4\widetilde{F}_{,r}+h_5\widetilde{F}+h_6\widetilde{G}\,. \tag{20}$$

Explicit expressions for the set of coefficients f_i, g_i, h_i can be found in Appendix A. For $\chi\neq0$, the coefficients f_i, g_i, h_i have terms which are time-dependent trigonometric functions of Ωt and, as a result, each of the eqs. (18)–(20) is not a simple parabolic equation describing a pure diffusive phenomenon. In addition to a secular Ohmic decay, in fact, there will be a periodic modulation produced by the rotation of the star. This is evident if we look, for instance, at the coefficient f_1 in Appendix A and which is given by the sum of two terms. The first one is the constant "diffusion" coefficient responsible for the decay on a secular timescale. The second term, on the other hand, represents the correction due to the stellar rotation. The periodic modulation is produced by the trigonometric function $\tan\lambda$ and varies therefore on the dynamical timescale set by the rotation period of the star, P. The presence of these periodic terms spoils the parabolic character and makes the set of eqs. (18)–(20) a mixed hyperbolic-parabolic one.

Although the integration of eqs. (18)–(20) is complicated in the general case, we are here favoured by the fact that all of the terms proportional to Ω or to ω (i.e. all of the terms directly related to the stellar rotation) scale like σ^{-2} and that the electrical conductivity in realistic neutron stars is very high, ranging in the interval $10^{21}-10^{28}\mathrm{s}^{-1}$. As a result, the star's rotation period is about twenty orders of magnitude smaller than the secular timescale and can be ignored in the numerical solution of the equations. In practice then, we set all of the periodic time-varying terms to be constant coefficients and solve the set of eqs. (18)–(20) as a purely parabolic system. In this way we can capture the secular decay without having to pay attention to the high frequency modulation. In Section 4, where we discuss the results of the numerical integration of the induction equations (18)–(20), we will also comment on the validation of this procedure.

Another important aspect of the numerical solution is the use of the zero-divergence constrain equation (14). We do not need, in fact, to integrate in time all of the eqs. (18)–(20) but can restrict the evolution to two of them and obtain, at each timestep, the remaining unknown radial eigenfunction from the solution of the constraint equation (14). Adopting this strategy in the numerical solution reduces the computational costs and, most importantly, enforces a constrained solution at each timestep.

Having three induction equations, we can follow the decay of each component of the magnetic field separately. The physically relevant quantity is however the modulus of the magnetic field which, in the locally flat spacetime of the ZAMO observer, is simply given by $|B| = [(B^{\hat{r}})^2 + (B^{\hat{\theta}})^2 + (B^{\hat{\phi}})^2]^{1/2}$. The evolution of this quantity, evaluated at the surface of the star, is the one that will be discussed in the remainder of the paper.

3.3 The Initial Value Problem

The consistent solution of the initial value problem for the general relativistic decay of the magnetic field in a rotating neutron star suffers from two difficult aspects. The first one is that at present the initial topology and location of the magnetic field in neutron stars can be only argued on the basis of some assumptions, so that the magnetic field can either permeate the entire star, or be confined in a layer close to the stellar surface. The first configuration is more plausible if the magnetic field is the final product of a dynamo action amplification (see Thompson & Duncan, 1993), while the second field configuration is more realistic in a scenario in which the magnetic field is originated by thermoelectric effects (Urpin *et al*, 1986; Wiebicke & Geppert, 1996). We here focus our attention mostly on the case of a magnetic field permeating the entire star, but in Section 4 we also show how the decay of the magnetic field depends on the depth of penetration inside the star, when simplified assumptions on the microphysics at the crust-core boundary are made.

The second difficult aspect of the initial value problem concerns the definition of an initial configuration which is also solution of the general relativistic Maxwell equations. A possible approach to this problem is the one proposed by Geppert *et al* (2000) (but see also Sang and Chanmugan, 1987), who have considered the initial magnetic field to be described by Stoke functions that represent, in flat spacetime, a class of exact solutions of the induction equation. In this case, the radial eigenfunction $\widetilde{F}(r)$ at the initial time can be obtained from

$$\widetilde{F}(r,t) \quad = \quad B_0 \left[\frac{\sin(\pi r/R)}{\pi^2 r/R} - \frac{\cos(\pi r/R)}{\pi} \right] e^{-\pi c^2 t/4\sigma R^2}, \qquad\qquad 0 \le r \le R\,, \tag{21}$$

for $t = 0$, where B_0 is the initial surface magnetic field at the magnetic pole. Because eq. (21) is not a solution of the general relativistic Maxwell equations, one expects an initial error being introduced in the solution of the induction equations, but also that this error should disappear rapidly as the solution tends to the one satisfying the Maxwell equations.

To circumvent the problem of an inaccurate solution during the initial stages of the evolution and in order to calculate an initial magnetic field which is solution of the relativistic Maxwell equations, we here treat the initial magnetic field as the one permeating a perfectly conducting medium. In this case, Rezzolla et al. (2001a, 2001b) have shown that consistent radial eigenfunctions can be obtained after solving the following set of equations [see (71)–(73) of paper I]

$$\widetilde{F}_{,r} + 2e^{\Lambda-\Phi}\widetilde{G} = 0\,, \tag{22}$$

$$\widetilde{H}_{,r} + \frac{e^{\Phi+\Lambda}}{r^2}\widetilde{F} = 0\,, \tag{23}$$

$$\widetilde{H} - \widetilde{G} = 0\,. \tag{24}$$

In particular, combining eqs. (22) and (23), we obtain a second-order differential equation for the unknown radial eigenfunction $\widetilde{F}$

$$\frac{d^2\widetilde{F}}{dr^2} + \frac{d}{dr}(\Phi - \Lambda)\frac{d\widetilde{F}}{dr} - 2e^{2\Lambda}\frac{\widetilde{F}}{r^2} = 0\,. \tag{25}$$

Equation (25) can be solved as a two-point boundary value problem after specifying values for the magnetic field at the edges of the numerical grid. More specifically, the initial magnetic field at the inner edge of the grid is chosen to be zero both when the magnetic field permeates the whole star and when it is confined to a crustal layer. On the other hand, the initial magnetic field at the outer edge of the grid is chosen to match a typical surface magnetic field for a neutron star and is therefore set to be $B_0 = 10^{12}$ G. Once the initial profile for $\widetilde{F}$ has been calculated through eq. (25), the corresponding initial values for $\widetilde{G}$ and $\widetilde{H}$ follow immediately from eqs. (22) and (24). As a comparison, we have also solved the induction eqs. (18)–(20) using as initial condition eq. (21) and the corresponding eigenfunctions $\widetilde{G}$ and $\widetilde{H}$ again as computed from the conditions (22) and (24).

Fig. 1 shows the initial values for the two different prescriptions and, in particular, with a solid line the initial profile as obtained through the solution of the Maxwell eqs. (25) and with a dashed line the Stoke profile given by expression (21). The noticeable differences between the two initial profiles provide a simple explanation of why the use of Stoke's function produces an initially inaccurate evolution (cf. Fig. 2).

The use of the strategy discussed above for the calculation of the initial value problem clearly requires the solution of an additional set of equations but it has the advantage of removing the adjustment of the solution during the initial stages of the decay and provides a more accurate estimate of the magnetic field decay. A discussion of this as well as a comparison with evolutions performed with the Stoke function will be discussed in Section 4. Finally, another aspect worth stressing is that by using eq. (25) we also automatically satisfy appropriate boundary conditions at the surface of the star.

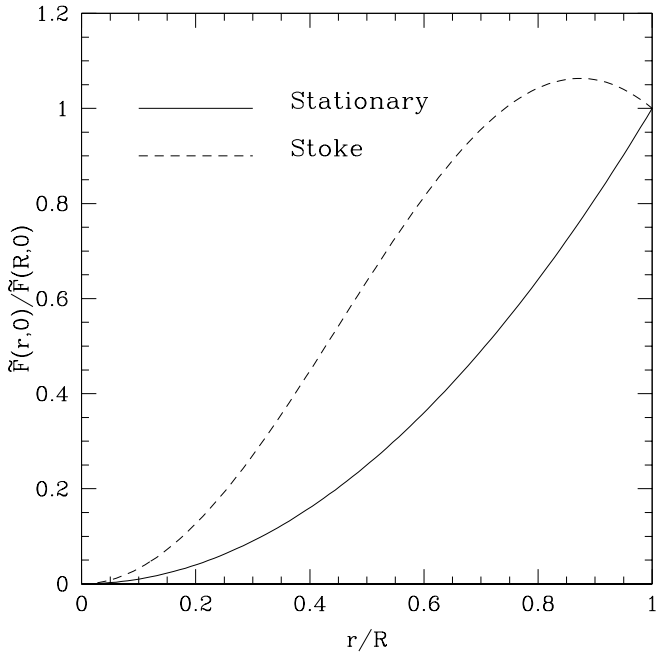

Figure 1. Possible initial values for the radial eigenfunction $\widetilde{F}$ of the radial component of the magnetic field normalized to the value at the surface, shown as a function of the radial position in the star. The solid line represents the radial eigenfunction $\widetilde{F}$ as obtained from the integration of the Maxwell eqs. (25), while the dashed line represents the Stoke profile (21).

3.4 Boundary Conditions

In order to correctly solve the induction equations (18) – (20), it is essential that appropriate boundary conditions are specified both at the inner edge of the computational domain as well as at the stellar surface.

As for the initial value problem, the inner boundary condition imposed during the evolution is that of a zero magnetic field and is applied both when the magnetic field permeates the whole star and when it is confined to the crust. In the first case, this choice guarantees a regular behaviour of the radial eigenfuctions at the origin, while it reflects the absence of magnetic field below the crust in the second case. The evolution of the magnetic field has shown to be quite sensitive to the boundary conditions imposed at the stellar surface, but proper boundary conditions can be derived if we assume that there are no electrical currents on the surface and impose a matching between the external and the internal solutions of the magnetic field. The radial eigenfunctions $F(r)$, $G(r)$, and $H(r)$ outside the slowly rotating relativistic star have been derived in paper I [see eqs. (90) – (92) therein] and are given by

$$\widetilde{F}(r) = -\frac{3r^2}{4M^3}\left[\ln N^2 + \frac{2M}{r}\left(1+\frac{M}{r}\right)\right]\mu\,, \tag{26}$$

$$\widetilde{G}(r) = \frac{3N^2}{4M^2}\left[\frac{r}{M}\ln N^2 + \frac{1}{N^2} + 1\right]\mu\,, \tag{27}$$

$$\widetilde{H}(r) = \widetilde{G}(r)\,, \tag{28}$$

where $N(r) \equiv (1-2M/r)^{1/2} = e^{\Phi}$ and μ is the magnetic dipole moment. Since the constraint expressed by eq. (22) holds also on the stellar surface, we then have

$$\widetilde{F}_{,r}\Big|_R + 2e^{\Lambda-\Phi}\widetilde{G}(R) = 0\,. \tag{29}$$

Moreover, when electrical surface currents are not present, we can use eq. (26) and (27) to express $\widetilde{G}(R)$ as

$$\widetilde{G}(R) = -\left(\frac{\widetilde{N}^2 M}{R^2}\right)\frac{R\ln\widetilde{N}^2/M + 1/\widetilde{N}^2 + 1}{\ln\widetilde{N}^2 + 2M\left(1+M/R\right)/R}\widetilde{F}(R)\,, \tag{30}$$

where $\widetilde{N} \equiv N(r=R)$. Straightforward calculations allow to conclude that

$$R\widetilde{F}_{,r}\Big|_R = \Pi(\eta)\widetilde{F}(t,R)\,, \tag{31}$$

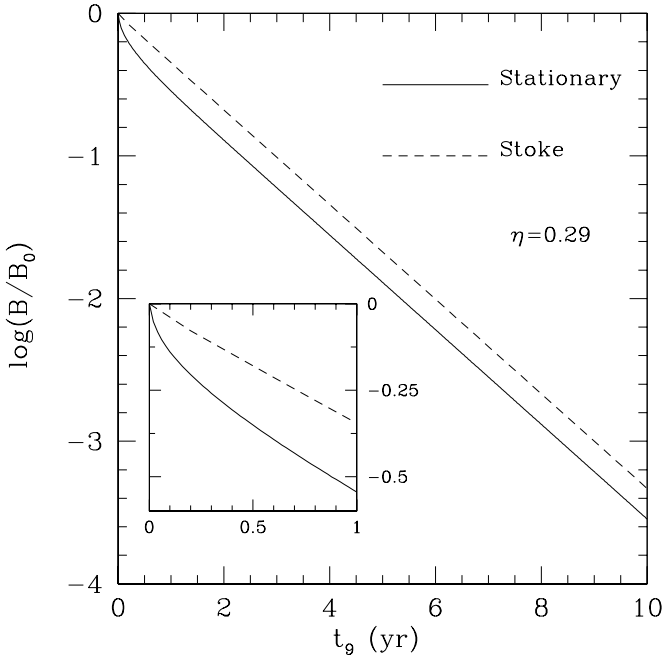

Figure 2. Difference in the decay of the magnetic field when a consistent initial magnetic field is used (solid line) or when a Stoke function is used as initial condition (dashed line). The inset shows a magnification of the evolution during the first 10^9 yr. Here $\sigma = 10^{25} s^{-1}$ and $P = 10^{-3} s$. See the main text for a complete discussion.

where $\Pi(\eta)$ is a constant given by

$$\Pi(\eta) \equiv \frac{4\ln(1-\eta) + 2\eta(2-\eta)/(1-\eta)}{2\ln(1-\eta) + 2\eta + \eta^2}\,, \tag{32}$$

with $\eta \equiv 2M/R$ being the compactness of the star. The corresponding boundary conditions for $\widetilde{G}$ and $\widetilde{H}$ are then easily obtained by means of (28) and (30).

Note that eq. (31) coincides with the boundary condition used by Geppert *et al* (2000) in the case of a static, spherically symmetric background geometry. This is due to the fact that, as discussed in paper I, the corrections to the components of the magnetic field enter at orders higher than the first one in Ω. Details on the numerical implementation of the surface boundary conditions are presented in Appendix B.

4 NUMERICAL RESULTS

In order to integrate the set of induction eqs. (18)–(20), we have built a numerical code which implements the Crank-Nicholson implicit evolution scheme and which provides second order accuracy both in space and in time (see Morton & Mayers, 1994). The accuracy of the code has been checked by computing the time evolution of eq. (21) which provides, in a flat spacetime, an exact solution of the induction equation. The results obtained indicate that the relative error between the numerical and the analytic solutions over a timescale of three Newtonian Ohmic times $\tau_{\rm ohm} \equiv 4\pi R^2\sigma/c^2$, is always below 0.5% for the level of grid resolution usually implemented in our calculations.

Established the consistency and accuracy of the code, we have proceeded to solve the general relativistic induction equations for our relativistic rotating star. As mentioned in Section 3.2, if the inclination angle between the rotation axis and the dipolar magnetic moment is nonzero, the secular decay has a periodic modulation due to the stellar rotation. We have also discussed that because the decay timescale and the rotation period timescale differ for about twenty orders of magnitude, we can neglect the time dependence (which is $\propto \sin\lambda$) contained in each of the coefficients f_i, g_i, h_i and set the periodic terms equal to an arbitrary constant value. To validate this procedure and verify that the periodic modulation does not affect the secular evolution, we have solved the induction equations using different constant coefficients and found that the secular results are indeed insensitive to the value chosen for the constant coefficients. We have also followed the solution of the complete set of eqs. (18)–(20) (i.e. not considering the time-periodic terms as constant) on a timescale which is longer than the dynamical timescale but still much smaller then the secular one. Also in this case we have verified that the modulated evolution, which is superimposed on the secular one, shows the small decrease corresponding to the secular decay.

Our discussion of the results starts by comparing the evolution of eqs. (18)–(20) for the two different prescriptions of the initial value problem discussed in Sect. 3.2 (cf. Fig. 1) for our fiducial neutron star. Before presenting the results of the comparison, it is useful to discuss

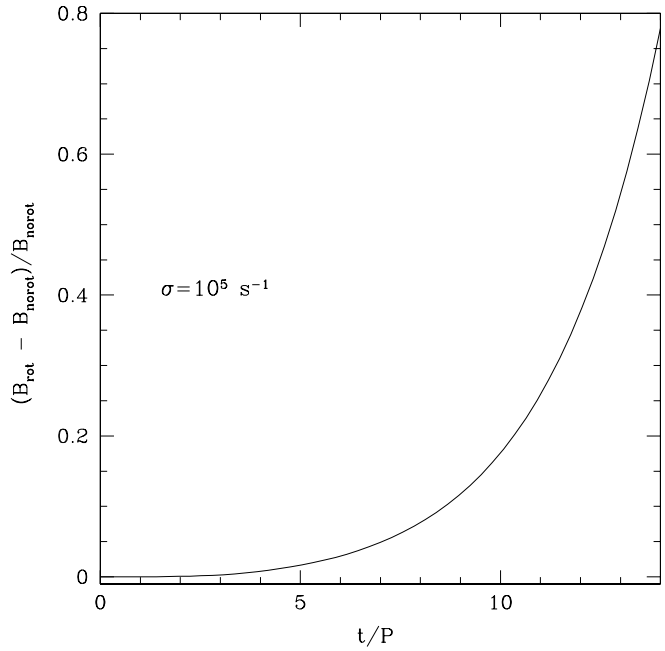

Figure 3. Relative difference in the evolution of a magnetic field in a nonrotating star $B_{\rm nonrot}$ and in a rapidly rotating one $B_{\rm rot}$. The electrical conductivity is here set to be $\sigma = 10^5$ s^{-1}, while the star been set to have a period $P = 10^{-3}$ s.

briefly the subtleties related to the measure of the magnetic field time decay; as will become apparent later, this is an important issue which might lead to seemingly conflicting results. The gauge freedom inherent in the theory of General Relativity allows for the choice of arbitrary observers with respect to which the measure of physically relevant quantities is made. The choice of a certain class of observers might rely on the mathematical advantages that this class may have, but not all observers are physically suitable observers. Locally inertial observers are certainly preferable and in a rotating spacetime, as the one considered here, ZAMO observers represent a natural choice. Of course, there is is an infinite number of such observers, each one performing his own measure of the magnetic field decay, so that one should then select a specific set of inertial observers on the basis of physical considerations. The results presented in this paper will be referred to a ZAMO observer on the surface of the star and at a latitude $\theta = \pi/2$. The values of the magnetic field measured by this observer and its time evolution can then be converted to the equivalent ones measured by other ZAMOs at different radial and polar positions through simple transformations involving the difference in the red-shifts and latitudes. Once the choice of a suitable class of inertial observers is made, it is also important that the results of the general relativistic magnetic field decay are expressed using appropriate units. In their work, Geppert *et al* (2000) have quantified the decay of magnetic field in a relativistic constant density, nonrotating star in terms of the Newtonian Ohmic time. As we shall show below, while this choice is acceptable for a constant density star, it could be misleading in general.

The two solutions of eqs. (18)–(20) are presented in Fig. 2 and show the decay of the magnetic field , rescaled on a timescale $t_9 \equiv 10^9$ yr. It is interesting to note that while the asymptotic decay rates of the magnetic field are almost the same for the two approaches, a final difference emerge. This is because when using Stoke's function as initial data, the evolution does not satisfy Maxwell's equations during the initial stages (see the small inset in Fig. 2), but settles onto a constrained solution only after that time. Moreover, the outer boundary conditions expressed by eqs. (30) and (31) cannot be satisfied exactly by Stoke's function and this introduces an additional error. As a result, after a time $t \sim t_9$ yr, the two solutions differ of about 45%, but this difference does not grow further in time.

Next, we discuss the effects introduced by the rotation of the star and of the spacetime. In this case it is worth distinguishing the interest in finding a general relativistic correction, from the impact that these corrections actually have on the magnetic field decay in a realistic rotating neutron star. As discussed in Section 3.2, in fact, the high value of the electrical conductivity in realistic neutron stars tends to make the general relativistic corrections due to rotation rather minute. In particular, we have found that when considering an electrical conductivity $\sigma = 10^{25}$ s^{-1} in a rapidly rotating neutron star with one millisecond rotation period, the relative difference in the magnetic field after $15\ t_9$ yr is only one part in 10^{12}. Nevertheless, general relativistic, rotation-induced corrections have an interest of their own and these corrections can be more easily appreciated if smaller (and therefore less realistic) values of the electrical conductivity are considered. In Fig. 3 we show the relative difference in the evolution of a magnetic field in a nonrotating star, $B_{\rm nonrot}$, and in a rapidly rotating one with a millisecond period, $B_{\rm rot}$. In this case and just for illustrative purposes, an electrical conductivity $\sigma = 10^5$ s^{-1} has been considered. As can be appreciated from the figure, the corrections due to the rotation *decrease* the rate of decay of the magnetic field and after a few rotation periods, the fastly rotating star will maintain a magnetic field which is about a factor of two larger than the one calculated for the nonrotating star. Overall, the results obtained indicate that General Relativity does introduce, through the rotation of the spacetime, new corrections to the evolution

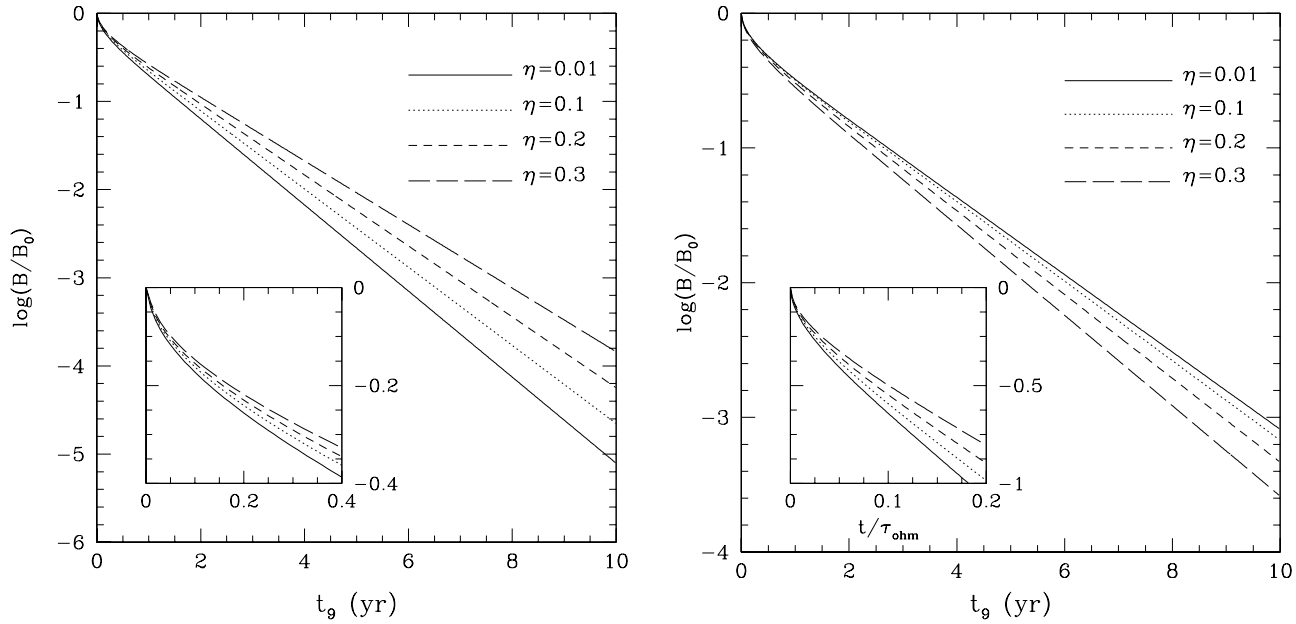

Figure 4. Decay of the surface magnetic field as measured by a ZAMO observer on the surface of the star at a latitude $\theta = \pi/2$, expressed on a timescale $t_9 \equiv 10^9$ yr. The left panel refers to a constant density stellar model and shows an asymptotic decay rate of the magnetic field which is *decreasing* for increasing values of the stellar compactness. The inset in the left panel focuses on the initial stages of the evolution when the decay is larger. The right panel, on the other hand, refers to an $N = 1$ polytropic stellar model and shows an asymptotic decay rate which is *increasing* for increasing values of the stellar compactness. Here the central density is the free parameter determining the stellar compactness. The small inset in the right panel of the figure shows how the use of an Ohmic timescale as normalizing unit can lead to erroneous interpretations.

of the magnetic field, slightly *decreasing* its decay rate. This effect, however, is usually hidden by the high electrical conductivity of the stellar medium and can be neglected in general. The results discussed above depend also on the inclination between the rotation axis and the magnetic dipole moment, with the decrease rate being larger for larger inclination angles. In particular, for $\chi = \pi/2$, the residual magnetic field after $10\, t_9$ yr is smaller of a factor two as compared to the corresponding magnetic field for an inclination $\chi = 0$.

Next, we compare the results of our calculations for a polytropic relativistic star with those for a constant density star. This will provide a first qualitative estimate of the importance of the metric functions in the actual evolution of the magnetic field. The results are presented in Fig. 4 with the left panel referring to a constant density model and the right one to our fiducial polytropic model.

In the case of a constant-density star, we confirm the results obtained by Geppert *et al* (2000) and find that the evolution of the magnetic field approaches an exponentially decaying behaviour, with an asymptotic decay rate which is generally *decreasing* with increasing stellar compactness. The inset in the left panel of Fig. 4 shows in more detail the initial stages of the magnetic field decay and allows to appreciate that the magnetic field evolution is initially following an exponential decay with decay rates which are quite large but that then reach an asymptotic value after about 10^8 yr (Geppert *et al* 2000).

In the case of a polytropic star, on the other hand, the results in the right panel of Fig. 4 show a behaviour which is the opposite to the one encountered for a constant density model and that the asymptotic decay rate of the magnetic field is *increasing* with increasing stellar compactness. When a uniform electrical conductivity is used, the explanation behind the two distinct behaviours has to be found in the deviations that emerge in the internal spacetime for the two stellar models and in particular in the first radial derivatives of the metric functions Φ and Λ [cf. eqs. (2) – (3)]. These deviations produce sensible quantitative differences in the coefficients of eqs. (18) – (20) (see the Appendix for the explicit form of the coefficients) which are then responsible for the increase in the decay rate. It should also be remarked that the behaviour shown in the left panel could be easily reproduced, also in the case of a polytropic model, by means of a suitably defined electrical conductivity. In other words, the results presented in Fig. 4 underline that a definitive conclusion on the general relativistic evolution of the magnetic field cannot be drawn until a more realistic treatment of the electrical conductivity and of the equation of state is made.

The inset in the left panel of Fig. 4 can be used to explain the comment made above on the use of relevant normalization units. In the inset, in fact, we have plotted the same evolution shown in the main panel but with the time being normalized in terms of the Newtonian Ohmic time. Note that when we do so, the overall behaviour is inverted and the decay rate of the magnetic field in now decreasing for increasing stellar compactness. This is clearly incorrect and the misleading behaviour is due to the fact that the concept of an Ohmic time is a purely Newtonian one and is therefore justified only in a Newtonian context. A more suitable normalizing unit for a nonrotating relativistic star would be the general relativistic analogue of the Newtonian Ohmic time: $\widetilde{\tau}_{\rm ohm} \equiv 4\pi R^2 e^{2\Lambda-\Phi}\sigma/c^2$ as can be derived from eqs. (18) – (20) in the limit $\Omega = 0$. Using this normalization, we would recover the correct behaviour, with a magnetic field asymptotic decay rate generally *increasing* with stellar compactness. Unfortunately the validity of $\widetilde{\tau}_{\rm ohm}$ is limited to nonrotating stellar models only. Because of the

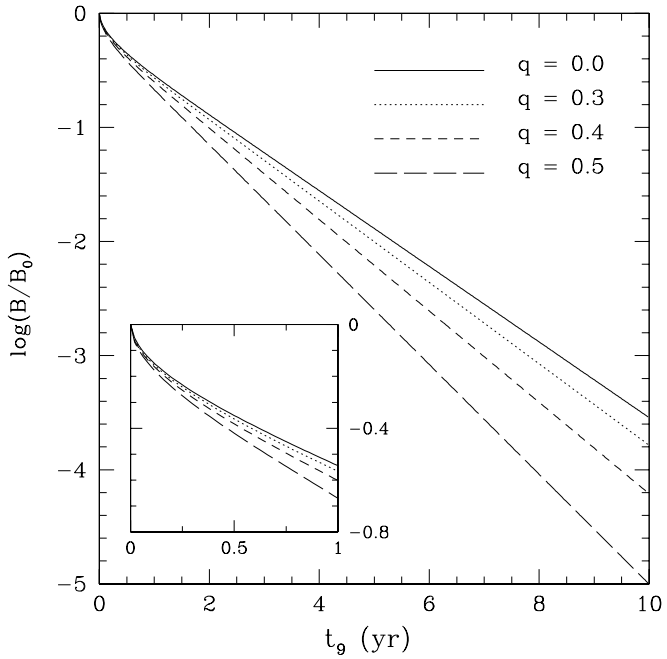

Figure 5. Decay of the surface magnetic field when the magnetic field does not penetrate the whole star. The different curves refer to different values of the parameter $q \equiv R_{\rm IN}/R$, with $R_{\rm IN}$ being the inner radius of the stellar shell where the magnetic field is confined.

difficulties of defining an Ohmic timescale for the induction equations of a relativistic rotating star, we measure the magnetic field evolution simply in terms of the time measured by our ZAMO observer.

Finally, we discuss the differences introduced in the decay of the magnetic field when the latter is confined to a spherical shell between an inner radius $R_{\rm IN}$ and the surface of the star. In this case, the initial values for the radial eigenfunctions are calculated self-consistently along the procedure discussed in Section 3.3. In Fig. 5 we show the evolution of the magnetic field in our fiducial neutron star for different values of the parameter $q \equiv R_{\rm IN}/R$. Note that decreasing the volume in which the magnetic field is confined has the effect of *increasing* the decay rate of the magnetic field so that if the initial magnetic field permeates about 90% of the stellar volume ($q = 0.5$), the residual surface magnetic field after $10\ t_9$ yr is about a factor thirty smaller than in the case the magnetic field permeates the whole star ($q = 0$). Although our analysis does not take into account the microphysics of the stellar interior and in particular the role played by the chemical composition and by the temperature, it confirms the Newtonian results of Urpin and & Konenkov (1997) and those of Page *et al* (2000), who have shown that the magnetic field decay is slower for deeper magnetic field penetration. Because this behaviour mimics the increase in the decay rate produced by an increasing compactness of the stellar model, it is essential to be able to determine, prior to observations, the geometry and location of the magnetic field within the neutron star and to distinguish the different contributions to the overall magnetic field decay.

5 CONCLUSIONS

In a recent paper, Rezzolla *et al* (2001a) have considered the general relativistic description of the electromagnetic fields of a slowly rotating, magnetized and misaligned neutron star. If the stellar medium has a finite electrical conductivity it was shown that the stellar rotation removes the degeneracy in the evolution equations for the magnetic field and that three distinct induction equations need to be solved to account for the decay of the stellar magnetic field. In this paper we have solved numerically the general relativistic induction equations derived in paper I, investigating the effects of different rotation rates, different inclination angles between the magnetic moment and the rotation axis, as well as different values of the electrical conductivity. The aim of these numerical calculations is that of quantifying the corrections induced by general relativistic effects (both due to spacetime curvature and to the stellar rotation) on the evolution of the magnetic field of a slowly rotating neutron star.

In order to single out purely general relativistic effects from those due to the microphysics of the Ohmic dissipation, we have considered a simplified physical description of the neutron star. In particular, the star has been modelled as a polytrope rotating with a fiducial period of one millisecond, the electrical conductivity has been considered to be uniform inside the star and we have not included a treatment to consider the evolution of the stellar rotation and temperature (see Page *et al* 2000). On the other hand, special attention has been paid to a consistent solution of the initial value problem and we have considered as initial magnetic field the stationary solution of the general relativistic Maxwell equations. In this way we have avoided the use of initial magnetic field configurations that are only approximate solutions of the Maxwell equations (i.e. solutions of the Maxwell equations only in the limit of flat spacetime). Besides eliminating an initial error during the initial

stages of the magnetic field decay, our prescription for the initial value problem also provides a more accurate solution of the Maxwell equations.

The results of our computations have shown that there exist general relativistic, rotation-induced corrections to the evolution of the magnetic field. These effects generally produce a *decrease* in the rate of magnetic field decay. However, their contribution is masked by the high value of the electrical conductivity in realistic neutron stars and can be neglected in general. Our calculations also indicate that general relativistic effects not induced by the stellar rotation can modify the time evolution of the magnetic field in a magnetized star. Such effects are closely related to the properties of the spacetime internal to the star and for a polytropic stellar model with uniform electrical conductivity these effects generally *increase* the decay rate of the field. The validity of this conclusion is however limited. Density gradients are in fact expected in a realistic star and these will affect the behaviour of the electrical conductivity which, in turn, will influence the decay of the magnetic field.

Our conclusions are that the general relativistic evolution of the magnetic field in rotating neutron stars can be studied with confidence already in a nonrotating background spacetime. However, the role of a curved background spacetime on the decay of the magnetic field can be fully assessed only when the details of both a realistic equation of state and of a realistic electrical conductivity are carefully taken into account. This will be the subject of future work.

Acknowledgments

We would like to thank Bobomurat Ahmedov and John Miller for the numerous discussions. We have also appreciated the useful comments of the referee, Ulrich Geppert. Support for this research comes from the Italian MURST and by the EU Programme “Improving the Human Research Potential and the Socio-Economic Knowledge Base” (Research Training Network Contract HPRN-CT-2000-00137).

REFERENCES

Ahmedov, B. J., 1999. Phys. Lett. A, 256, 9.
Anderson, J. L., Cohen, J. M., 1970. Astrophys. Space Science, 9, 146.
Duncan, R. C., Thompson, C., 1992. ApJ, 392, L9.
Geppert, U., Urpin V., 1994, MNRAS , 271, 490.
Geppert, U., Page, D., Zannias, T., 2000. Phys. Rev. D, 61, 123004
Ginzburg, V. L., Ozernoy, L. M., 1964. Zh. Eksp. Teor. Fiz., 47, 1030.
Gupta, A., Mishra, A., Mishra, H., Prasanna, A. R., 1998, Class. Quantum Grav. 15, 3131.
Hartle, J. B., 1967. ApJ, 150, 1005.
Hartle, J. B., Thorne, K. S., 1968. ApJ, 153, 807.
Konenkov, D., Geppert, U., 2001, MNRAS, 325, 426.
Konno K., Kojima Y., 2000, Prog. of Theor. Phys. 104, 1117.
Morton, K. W., Mayers, D. F., 1994, *Numerical Solution of Partial Differential Equations*, Cambridge University Press
Miller, J. C., 1977. MNRAS 179, 483.
Oppenheimer, J. R., Volkoff, G.M., 1939. Phys. Rev., 55, 374.
Page, D., Geppert, U., Zannias, T., 2000, Astron. Astrophys., 360, 1052.
Petterson, J. A., 1974. Phys. Rev., D10, 3166.
Prasanna, A. R., Gupta, A., 1997, Il Nuovo Cimento B, 112, 1089.
Rezzolla, L., Ahmedov, B. J., Miller, J. C., 2001a, MNRAS, 322, 123
Rezzolla, L., Ahmedov, B. J., Miller, J. C., 2001b, Found. of Phys., 31, 1051.
Salgado, M., Bonazzola, S., Gourgoulhon, E., Haensel, P., 1994. Astron. Astrophys. 291, 155.
Sang Y. and Chanmugam G., 1987, ApJ, 323, L61.
Sengupta, S., 1995. ApJ, 449, 224.
Sengupta, S., 1997. ApJ, 479, L133.
Thompson, C., Duncan, R., 1993., ApJ, 408, 194.
Tolmann, R.C., 1939. Phys. Rev., 55, 364.
Urpin, V., Konenkov, D., 1997. MNRAS, 292, 167.
Wasserman, I., Shapiro, S. L., 1983. ApJ, 265, 1036.
Wiebicke, H. J., Geppert, U., 1996. Astron. Astrophys. , 309, 203.

APPENDIX A1: THE NUMERICAL SOLUTION OF THE INDUCTION EQUATIONS

In this Appendix we provide the explicit expressions for the coefficients f_i, g_i, h_i appearing in the new form of the induction equations (18) – (20)

$$
\begin{aligned}
f_1 &= \frac{c^2 e^{\Phi-2\Lambda}}{4\pi\sigma} - \frac{c^2 e^{-2\Lambda}}{(4\pi\sigma)^2}\omega\tan\lambda(1-2\sin^2\theta)\ ,\\
f_2 &= \frac{c^2 e^{\Phi-2\Lambda}}{4\pi\sigma}(\Phi_{,r}-\Lambda_{,r}) + \frac{c^2 e^{-2\Lambda}}{(4\pi\sigma)^2}\tan\lambda(1-2\sin^2\theta)(\Omega\Phi_{,r}+\omega\Lambda_{,r}-\omega_{,r})\ ,\\
f_3 &= \frac{-2c^2 e^{\Phi}}{4\pi\sigma r^2} - \frac{2\omega c^2}{(4\pi\sigma r)^2}\sin\theta\frac{\Psi_3}{\Psi_1}\ ,\\
f_4 &= \frac{-2c^2 e^{-\Phi-\Lambda}}{(4\pi\sigma)^2}\omega\sin\theta\frac{\Psi_3}{\Psi_1}\ ,\\
f_5 &= \frac{2c^2 e^{-\Phi-\Lambda}}{(4\pi\sigma)^2}\tan\lambda(1-2\sin^2\theta)(\Phi_{,r}(\Omega+\omega)-\omega_{,r})\ ,\\
f_6 &= \frac{-2c^2 e^{-\Phi-\Lambda}}{(4\pi\sigma)^2}\omega\tan\lambda(1-2\sin^2\theta)\ ;
\end{aligned}
$$

$$
\begin{aligned}
g_1 &= \frac{c^2 e^{\Phi-2\Lambda}}{4\pi\sigma} - \frac{c^2 e^{-2\Lambda}}{(4\pi\sigma)^2}\omega\cos\theta\frac{\Psi_3}{\Psi_2}\ ,\\
g_2 &= -\frac{c^2 e^{\Phi-2\Lambda}}{4\pi\sigma}\Lambda_{,r} + \frac{c^2 e^{-2\Lambda}}{(4\pi\sigma)^2}\cos\theta\frac{\Psi_3}{\Psi_2}\left[\Phi_{,r}(2\omega-\Omega)+\omega\Lambda_{,r}-2\omega_{,r}\right]\ ,\\
g_3 &= \frac{c^2 e^{\Phi}}{(4\pi\sigma)r^2}\frac{\cos\theta\sin\chi}{\sin^2\theta\Psi_2}(\cos\lambda+\frac{\omega e^{-\Phi}}{4\pi\sigma}\sin\lambda)\ ,\\
&\quad -\frac{c^2 e^{-2\Lambda}}{(4\pi\sigma)^2}\cos\theta\frac{\Psi_3}{\Psi_2}\left[\omega_{,rr}-\omega_{,r}(\Lambda_{,r}+2\Phi_{,r})+\Phi_{,rr}(\Omega-\omega)+(\omega-\Omega)(\Phi_{,r}^2+\Phi_{,r}\Lambda_{,r})\right]\ ,\\
g_4 &= \frac{c^2 e^{\Phi-\Lambda}}{(4\pi\sigma)r^2}\left[e^{\Phi}-\frac{\omega}{4\pi\sigma}\cos\theta\frac{\Psi_3}{\Psi_2}\right]\ ,\\
g_5 &= \frac{c^2 e^{2\Phi-\Lambda}}{(4\pi\sigma)r^2}(\Phi_{,r}-\frac{2}{r}) - \frac{c^2 e^{\Phi-\Lambda}}{(4\pi\sigma r)^2}\cos\theta\frac{\Psi_3}{\Psi_2}(\omega_{,r}-\frac{2\omega}{r})\ ,\\
g_6 &= -\frac{c^2 e^{-2\Lambda}}{(4\pi\sigma)^2}\cos\theta\frac{\Psi_3}{\Psi_2}\left[\Phi_{,r}(\omega-\Omega)-\omega_{,r}\right]\ ,\\
g_7 &= -\frac{c^2 e^{-2\Lambda}}{(4\pi\sigma)^2}\cos\theta\frac{\Psi_3}{\Psi_2}\left[\Phi_{,rr}(\omega-\Omega)-\omega_{,rr}+\Phi_{,r}^2(\Omega-\omega)+\Phi_{,r}\Lambda_{,r}(\Omega-\omega)+\omega_{,r}(2\Phi_{,r}+\Lambda_{,r})\right]\ ;
\end{aligned}
$$

$$
\begin{aligned}
h_1 &= \frac{c^2 e^{\Phi-2\Lambda}}{4\pi\sigma}(1-\frac{\omega e^{-\Phi}}{4\pi\sigma}\cot\lambda)\ ,\\
h_2 &= \frac{c^2 e^{\Phi-2\Lambda}}{4\pi\sigma}\left[\frac{e^{-\Phi}}{4\pi\sigma}\cot\lambda(\omega\Phi_{,r}+\omega\Lambda_{,r}-\omega_{,r})-\Lambda_{,r}\right]\ ,\\
h_3 &= -\frac{c^2 e^{\Phi}}{(4\pi\sigma)r^2\sin^2\theta}\left(1-\frac{\omega e^{-\Phi}}{4\pi\sigma}\cot\lambda\right)\\
h_4 &= \frac{c^2 e^{2\Phi-\Lambda}}{(4\pi\sigma)r^2}\left[1-\frac{\omega e^{-\Phi}}{4\pi\sigma}\cot\lambda\right]\ ,\\
h_5 &= \frac{c^2 e^{2\Phi-\Lambda}}{(4\pi\sigma)}\left[(\Phi_{,r}-\frac{2}{r})(1-\frac{\omega e^{-\Phi}}{4\pi\sigma}\cot\lambda)+\frac{e^{-\Phi}\cot\lambda}{4\pi\sigma}(\omega\Phi_{,r}-\omega_{,r})\right]\ ,\\
h_6 &= \frac{c^2 e^{\Phi}}{(4\pi\sigma)r^2\sin^2\theta}\left(1-\frac{\omega e^{-\Phi}}{4\pi\sigma}\cot\lambda\right)\ .
\end{aligned}
$$

APPENDIX A2: IMPLEMENTING SURFACE BOUNDARY CONDITIONS

This Appendix shows how the surface boundary conditions expressed by equations (27) and (31) can be implemented in a numerical code. By adopting the standard finite-difference notation in which $u_j^n \equiv u(x_j, t^n)$ and assuming a uniform radial grid with J gridpoints, the finite difference form of eq. (31) is given by

$$\widetilde{F}_{J+1}^n - \widetilde{F}_{J-1}^n = 2\Pi(\eta)\Delta x\widetilde{F}_J^n/R, \tag{A1}$$

where $\Delta x = x_j - x_{j-1}$, $\Delta t = t^{n+1} - t^n$, The unknown value of $\widetilde{F}_J^{n+1}$, comes after introduction of (A1) into the Crank-Nicholson scheme, centered at J; lengthy but straigthforward calculation give

$$\widetilde{F}_J^{n+1} = \underline{\alpha(f_1^n \widetilde{F}_{J-1}^n + f_1^{n+1}\widetilde{F}_{J-1}^{n+1}) + \widetilde{F}_J^n\,[1 + f_3^n\Delta t/2 - f_1^n\alpha + \Pi(\eta)\alpha\Delta x(f_2^n\Delta x/2 + f_1^n)/R]} + \frac{f_4^n\alpha\Delta x(\widetilde{H}_{J+1}^n - \widetilde{H}_{J-1}^n)/2 + f_5^n\widetilde{G}_J^n\Delta t + f_6^n\alpha\Delta x(\widetilde{G}_{J+1}^n - \widetilde{G}_{J-1}^n)/2}{1 - f_3^{n+1}\Delta t/2 + f_1^{n+1}\alpha - \Pi(\eta)\alpha\Delta x(f_2^{n+1}/2\Delta x + f_1^{n+1})/R}, \tag{A2}$$

where $\alpha = \Delta t/\Delta x^2$. The are still two unknowns entering (A2), i.e. $\widetilde{G}_{J+1}^n$ and $\widetilde{H}_{J+1}^n$. However, they represent the external solution and by using eqs. (28) and (30), they can be written as

$$\widetilde{G}_{J+1}^n = \widetilde{H}_{J+1}^n = -\frac{\tilde{N}^2 M}{(R+\Delta x)^2}\frac{(R+\Delta x)\ln\tilde{N}^2/M + 1/\tilde{N}^2 + 1}{\ln\tilde{N}^2 + 2M\,(1 + M/(R+\Delta x))\,/(R+\Delta x)}\widetilde{F}_{J+1}^n, \tag{A3}$$

where $\tilde{N}$ is the value of N at $R + \Delta x$

$$\tilde{N} \equiv N\Big|_{R+\Delta x} = \left(1 - \frac{2M}{R+\Delta x}\right)^{1/2}. \tag{A4}$$

The updated values of $\widetilde{G}$ and $\widetilde{H}$ now follow immediately from (30) with time evolved value of F_J^{n+1} given by (A2).